Available online at www.sciencedirect.com
SCIENCE DIRECT
Journal of Catalysis 233 (2005) 276–287
JOURNAL OF CATALYSIS
www.elsevier.com/locate/jcat

Synthesis and characterization of divalent cobalt-substituted mesoporous aluminophosphate molecular sieves and their application as novel heterogeneous catalysts for the oxidation of cycloalkanes

P. Selvam *, S.K. Mohapatra

Solid State and Catalysis Laboratory, Department of Chemistry, Indian Institute of Technology-Bombay, Powai, Mumbai 400076, India

Received 19 December 2004; revised 24 April 2005; accepted 26 April 2005

Available online 6 June 2005

Abstract

Thermally stable divalent cobalt-substituted hexagonal mesoporous aluminophosphate, CoHMA molecular sieves were hydrothermally synthesized and systematically characterized by several analytical and spectroscopic techniques. XRD, TEM, ED, ICP-AES, TGA-DTA, N_2 sorption, DR-UV–vis, XANES, and NH_3-TPD studies showed isomorphous substitution of divalent cobalt in a tetrahedral framework of a mesoporous aluminophosphate matrix. Furthermore, the blue color of CoHMA, before and after thermal treatment, further confirmed the tetrahedral environment of divalent cobalt in the matrix. As a result, the CoHMA catalyst showed excellent activity for the oxidation of cycloalkanes, that is, cyclohexane, cyclooctane and cyclododecane, under mild reaction conditions. Unlike the many other cobalt-based heterogeneous catalysts reported so far, CoHMA does not show any dislodgement or segregation of cobalt with calcination or any other postsynthesis treatments. In this study, the performance of CoHMA was also compared with the cobalt-containing microporous aluminophosphate, that is, CoAPO-5 with AFI topology, as well as with both microporous and mesoporous analogues of cobalt silicate molecular sieves that have MFI or MCM-41 structures.

Keywords: Cobalt; Mesoporous; Aluminophosphates; CoHMA; Oxidation; Cycloalkanes; Cylcohexane; Cyclooctane; Cyclododecane

1. Introduction

Cobalt complexes/reagents in stoichiometric or catalytic amounts are known to be efficient in many homogeneous oxidation reactions. Among the cobalt-based homogeneous catalysts reported so far, the cobalt complexes of acetates, porphyrins, phthalocyanines, naphthenates, etc. have been extensively studied, with a special emphasis on the oxidation reaction of cyclohexane [1–7]. These catalysts are generally used either for the direct oxidation of cyclohexane to adipic acid or to K-A oil (a mixture of cyclohexanone and cyclohexanol), depending on the reaction conditions used. The cyclohexane oxidation process has been of particular interest in recent years for both academic and industrial reasons, because of the importance of the reaction products [8]. The lower stability of Co(III) salts/complexes compared with Co(II) has led to a wide range of applications of Co(II) catalysts in combination with weak organic acids, such as acetic acid [3,6,7,9]. However, the characteristics of these soluble homogeneous catalysts often pose a serious obstacle to their practical utility because of various problems like easy deactivation and difficulty in regeneration of the catalysts, and tedious procedures needed for the separation of the products. Therefore, it is important that the scientific community develop cleaner, environmentally benign, heterogeneous catalysts. In this regard, several cobalt-based heterogeneous catalysts have been proposed. One class of heterogeneous catalysts is composed of catalytically active metal complexes immobilized/anchored within a zeolite matrix with the so-called ship-in-a-bottle strategy [9]. Unfortunately, in many cases, the active metal complexes leach out under the reac-

* Corresponding author. Fax: +91 22 2572 3480.
E-mail address: selvam@iitb.ac.in (P. Selvam).

0021-9517/$ – see front matter
doi:10.1016/j.jcat.2005.04.036

tion conditions. The other class of heterogeneous catalysts, transition-metal-ion-incorporating molecular sieves or metal ion supported on inert matrix, has been used. However, the transition-metal-ion-incorporating molecular sieve approach has been found to be more effective compared with the supported methodology.

Consequently, the insertion of divalent cobalt has been reported for many microporous silicate and aluminophosphate molecular sieves [10–13], and these catalysts have been used for the oxidation of cyclohexane [14–21]. However, the small pore opening of these microporous molecular sieve catalysts restricts their application in processes dealing with bulky molecules, in addition to the typical problem of leaching of the active cobalt ions from the matrix. On the other hand, isomorphous substitution of divalent cobalt in various mesoporous silicate molecular sieves with MCM-41, MCM-48, and SBA-1 structures has been attempted. However, the large size and charge difference between divalent cobalt and tetravalent silicon and the compact network of the silicate framework have led to the formation of cobalt oxide clusters inside the mesopores of the framework structure [22–24]. Maschmeyer and co-workers [25,26] have encapsulated active homogeneous cobalt complexes inside mesopores, but the lifetime, activity, and heterogeneous nature of the catalyst remain to be addressed.

On the other hand, the successful synthesis of thermally stable metal-ion-incorporating, hexagonal mesoporous aluminophosphates (HMAs) has opened up new prospects and excellent opportunities in the area of heterogeneous catalysis [27]. In this paper, we present a detailed study of the synthesis and characterization of divalent cobalt-substituted hexagonal mesoporous aluminophosphates, CoHMA molecular sieves. The performance of the catalyst was evaluated for the oxidation reaction of cycloalkanes, that is, cyclohexane, cyclooctane, and cyclododecane, under mild reaction conditions. Furthermore, the catalytic activity of CoHMA was also compared with that of cobalt-containing mesoporous silicate (Co/MCM-41), microporous cobalt aluminophosphate (CoAPO-5), and cobalt silicalite-1 (Co/S-1) catalysts.

2. Experimental

2.1. Starting materials

The starting materials and their sources were phosphoric acid (85%; Qualigens), aluminum isopropoxide (97%; Merck), tetramethyl ammonium hydroxide (TMAOH, 25 wt% in water; Aldrich), cetyltrimethylammonium chloride (CTAC, 25 wt% in water; Aldrich), fumed silica (99.8%; Aldrich), cetyltrimethylammonium bromide (CTAB, 99%; Aldrich), sodium hydroxide (NaOH, 98%; Loba), cobaltous acetate ($Co(CH_3COO)_2{\cdot}4H_2O$, 99%; SD fine); triethylamine (99.5%; Thomas Baker), cobalt oxide (CoO, 70% Co; SD fine chemicals), pseudoboehmite (70%; Vista), tetrapropylammonium bromide (TPAB, 98%; Lancaster), cyclohexane (99.5%; Merck), *tert*-butyl hydroperoxide (TBHP, 70% aqueous solution; Lancaster), cyclooctane (99%; Lancaster), cyclododecane (99%; Lancaster), methyl ethyl ketone (MEK, 99.5%; SD fine), and glacial acetic acid (>99%; Fischer).

2.2. Synthesis

2.2.1. CoHMA

Phosphoric acid (1.4 ml) was first diluted with 11.7 ml water, and then 4.08 g aluminum isopropoxide was added with vigorous stirring, followed by the addition of cobalt acetate solution (0.378 g in 5 ml water). The mixture was kept under constant stirring at 343 K for 1 h, and then TMAOH (7.3 ml) was added dropwise. The slurry was kept under stirring for few hours. To this mixture CTAC (13.2 ml) was added dropwise and stirred for another 12 h. The pH was maintained at 10 with a final (molar) gel composition of $(1-x)\ Al_2O_3{:}P_2O_5{:}2x\ CoO{:}0.5\ (CTA)_2O{:}1.25\ (TMA)_2O{:}70\ H_2O$. By varying the value of x, we prepared several CoHMA compositions with different Co/[Al + P] (molar) ratios, that is, CoHMA(0.005), CoHMA(0.01), CoHMA(0.02), and CoHMA(0.04). The mixture was then transferred to a Teflon-lined autoclave and heated for crystallization at 373 K for 72 h. The resultant solid product was washed repeatedly with distilled water, filtered, and dried at 343 K for 12 h. The as-synthesized samples were then calcined at 823 K for 1 h under flowing N_2, followed by 2 h in O_2.

2.2.2. Co/MCM-41

The procedure adopted for the synthesis of Co/MCM-41 was as follows [22]. A solution of cobalt acetate (0.249 g) was made with 20 ml H_2O. Water glass was prepared with 1.2 g NaOH, 3 g SiO_2, and 13.2 ml H_2O. To water glass, a cobalt solution was added dropwise with vigorous stirring, and, subsequently, 0.3 ml H_2SO_4 and 4 ml H_2O were also added to the same. This solution is referred to as A. CTAB (7.2892 g) was added slowly to 22 ml H_2O and stirred for 30 min (solution B). Then solution B was slowly added to solution A and was stirred for 1 h to get a homogeneous gel with pH 11.3. The final gel (with a molar gel composition of $1\ SiO_2{:}0.020\ CoO{:}0.3\ Na_2O{:}0.08\ H_2SO_4{:}0.2\ (CTA)_2O{:}78\ H_2O$ ($Co/Si = 0.02$)) was kept in a Teflon-lined autoclave in an air oven at 393 K for 216 h. The pink solid products were washed, filtered, and dried for 12 h at 353 K. All of these as-synthesized products were calcined in a tubular furnace at 823 K for 2 h in a flow of N_2 and in air for 8 h.

2.2.3. CoAPO-5

In a typical procedure used to synthesize CoAPO-5 [10], 6.66 ml phosphoric acid was diluted with 20 ml water, and to this a cobalt acetate (1.582 g) solution in water (10 ml) was added. After a few minutes 7.14 g pseudoboehmite was added slowly, and the mixture was stirred for 2 h until a

homogeneous slurry was obtained. The organic template, triethylamine (10.45 ml), was finally added dropwise and was stirred vigorously for 2 h. The final gel (with a composition of 0.96 Al_2O_3:P_2O_5:0.75 TEA:0.08 CoO:17 H_2O ($Co/[Al+P] = 0.02$); pH 5.4) was subjected to a hydrothermal treatment at 463 K for 144 h in a Teflon-lined autoclave. The as-synthesized sample was calcined at 873 K under air for 10 h.

2.2.4. Co/S-1

Co/S-1 was synthesized hydrothermally with a procedure reported in the literature for Cr/S-1 [28] with a typical molar gel composition of 1 SiO_2:0.5 Na_2O:0.5 $(TPA)_2O$:0.020 CoO:100 H_2O ($Co/Si = 0.02$). First 4.0 g of fumed silica was dissolved in an aqueous NaOH solution (2.7 g in 30 ml water). To this, TPAB (17.7 g) was added slowly; then an aqueous solution of cobalt acetate (0.332 g in 10 ml water) was added, and the resulting gel was stirred for 3 h. The final gel was transferred into a Teflon-lined stainless-steel autoclave and was kept in an air oven for crystallization at 453 K for 86 h. The solid product obtained was washed, filtered, and dried at 373 K for 12 h. The as-synthesized samples were calcined at 823 K for 12 h under air.

2.3. Characterization

The as-synthesized and calcined samples were characterized by several analytical and spectroscopic techniques. Powder X-ray diffraction (XRD) patterns were recorded on a Rigaku-miniflex diffractometer with nickel-filtered Cu-K_α radiation ($\lambda = 1.5418$ Å) and a step size of 0.02°. Transmission electron micrograph (TEM) images and electron diffraction (ED) were recorded on a Philips 200 microscope operated at 160 kV. The sample (in fine powdered form) was dispersed in ethanol with sonication (Oscar ultrasonics); and a drop of the sample was placed on a carbon-coated copper grid (300 mesh; Sigma-Aldrich). The elemental analysis of the various samples was carried out by inductively coupled plasma–atomic emission spectroscopy (ICP-AES) with Labtam Plasma Lab 8440 equipment. Thermogravimetry/differential thermal analysis (TG-DTA) measurements were performed with ∼ 15 mg of the sample on a Dupont 9900/2100 TG/DTA system under a nitrogen atmosphere (40 ml min^{-1}) with a heating rate of 10 °C min^{-1}.

Surface area measurements were performed on a Sorptomatic-1990 instrument. Before measurement, the calcined sample was evacuated at 423 K for 12 h under vacuum (10^{-3} Torr; 1 Torr = 133.33 Pa). The specific surface area was calculated with the Brunauer–Emmett–Teller (SSA-BET) method, and the pore size was calculated with the Horvath–Kawazoe method. The pore volume was determined from the amount of N_2 adsorbed at $P/P_0 = 0.5$. Diffuse-reflectance ultraviolet and visible (DR-UV–vis) spectra were recorded on a UV-260 Shimadzu spectrophotometer (190–900-nm range) with Whatman-40 filter paper as a standard under ambient conditions. The XANES measurements were made with a focusing spectrograph of the Cauchois type with different radii of curvature and a laboratory source of X-rays. All of the experiments were performed at room temperature on finely powdered samples, which were mounted on cellophane adhesive tape. The spectra were background subtracted and normalized to 1.0 with respect to the point well above the edge. The first and second derivatives were also taken to bring out clearly the energy position and relative intensity of the spectral features of samples under investigation. It is important to note here that both DR-UV–vis and XANES studies were performed under air (dry condition; maintained with active silica in a closed sample vessel). Before measurements all of the samples were dried at 383 K for 2 h to remove adsorbed gas/water molecules.

The acidic behavior of the protonated catalyst was studied by temperature-programmed desorption of ammonia (TPDA). About 400 mg of sample was placed in quartz reactor and was activated at 823 K in air for 6 h followed by 2 h in helium (with a flow rate of 50 ml min^{-1}). Then the reactor was cooled to 373 K and maintained for another hour under the same conditions. Ammonia adsorption was carried out with a gas flow through the sample for 15–20 min at this temperature. Subsequently, it was purged with helium for an hour to remove the physisorbed ammonia. We carried out the desorption of ammonia heating the reactor to 873 K at a rate of 10 K min^{-1} with a temperature programmer (Eurotherm). The amount of ammonia desorbed was estimated with the aid of a thermal conducting detector (TCD) response factor for ammonia. The deconvolution was carried out with an MS-DOS program with Gaussian function. Unless otherwise stated, the catalyst used in the present study was $Co/[Al+P]$, and Co/Si ratio was 0.02.

2.4. Oxidation of cycloalkanes

2.4.1. Reaction procedure

The oxidation of cyclohexane (18 mmol) was carried out in the presence of 5 mmol initiator (MEK) at 373 K for 12 h under atmospheric pressure, with 50 mg of the catalyst, 18 mmol of oxidant (30% H_2O_2), and 10 ml of solvent (acetic acid). After the reaction, the catalyst was separated and the products were extracted with ether and analyzed by GC with a Carbowax column. The cyclohexane oxidation reaction was also carried out with various other solvents, such as methanol, tetrahydrofuran (THF), and acetone, under the same reaction conditions. Furthermore, the influence of different oxidants, such as air, oxygen, and *tert*-butyl hydroperoxide, on the reaction was investigated. Oxidation of cyclooctane (18 mmol) and cyclododecane (12 mmol) was carried out under conditions similar to those mentioned above for the cyclohexane reaction, but the only change made for cyclooctane and cyclododecane was that mixed solvents (5 ml acetic acid + 5 ml CH_2Cl_2) were applied to make a homogeneous reaction mixture.

2.4.2. Recycling studies

After the first run, the catalyst was filtered, washed with distilled water three times, dried in an air oven, activated at 773 K for 6 h, and used for the subsequent recycling studies.

2.4.3. Washing studies

The calcined catalyst (100 mg) was washed with 25 ml 1 M ammonium acetate for 12 h at room temperature with constant stirring. Then the catalyst was filtered, washed, dried, and activated at 773 K for 6 h. This catalyst is referred to as washed catalyst.

2.4.4. Filtrate and quenching studies

In the filtrate study, the reaction was carried out with the filtrate collected at room temperature, that is, the reaction mixture was cooled to room temperature and then filtered. On the other hand, in the quenching studies, the reaction was carried out with the filtrate collected while it was hot.

3. Results and discussion

XRD patterns of all of the as-synthesized CoHMA (Fig. 1) samples showed typical features characteristic of a mesoporous hexagonal system [29,30]. The reflections were well defined (see inset), indicating that the samples prepared here were of good quality. The average unit cell dimension (a_0) of the CoHMA samples was larger than the corresponding Co-free HMA. The a_0 values, however, increase with an increase in cobalt content in the structure (Table 1). This observation plausibly suggests the substitution/incorporation of Co(II) in the HMA matrix. It is clear from the figure that, upon calcination (removal of the surfactants), the unit cell shrinks for of all the samples because of framework contraction. Furthermore, higher order reflections disappeared, and only a single broad corresponding reflection was observed. Similar observations were also reported by most of the researchers working on HMA, who concluded that this may be due to finite size effects of very fine particle morphology or to the disordered structure [30–33]. Shown in Fig. 2 are the TEM image and ED pattern of calcined CoHMA. The former clearly indicates a disordered hexagonal array of mesopores, and the latter, the good quality of the samples. Fig. 3 depicts the XRD patterns of Co/MCM-41. The distinct profiles are typical of MCM-41 structure [30,34]. In general, the incorporation of a larger cation such as Co(II), with a crystal radius of 0.72 Å, in a silicate matrix, that is, Si(IV) in tetrahedral geometry with a crystal radius of 0.40 Å, is expected to increase the lattice parameter significantly. However, it can be seen from Table 1 that there was little

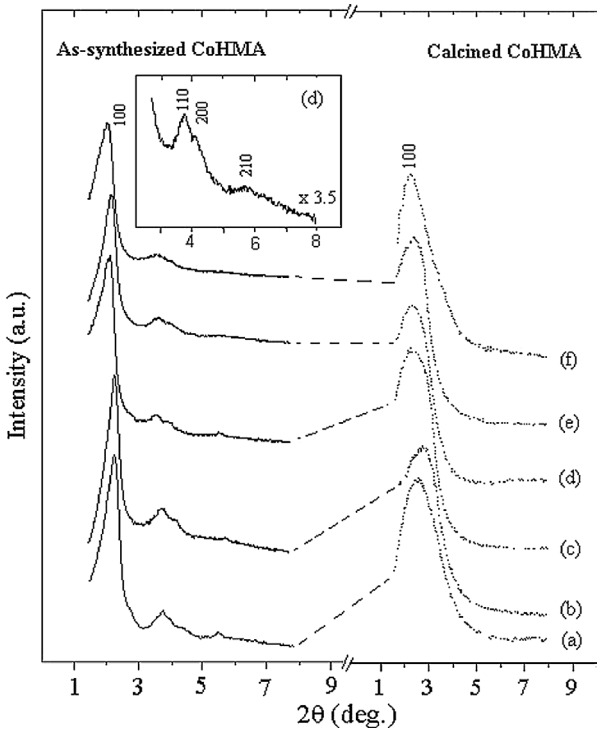

Fig. 1. XRD patterns (a) HMA; (b) CoHMA(0.005); (c) CoHMA(0.01); (d) CoHMA(0.02); (e) CoHMA(0.04); (f) calcined CoHMA(0.02) after reused. The inset shows the expanded diffraction pattern in the 2θ region 2°–8°.

Table 1
XRD and N_2 sorption data of various cobalt-containing HMA and MCM-41 samples

Sample[a]	XRD		N_2 sorption data		
	As-synthesized, a_0[b] (Å)	Calcined, a_0[b] (Å)	Surface area ($m^2\ g^{-1}$)	Pore volume ($ml\ g^{-1}$)	Pore diameter (Å)
HMA[c]	45.4	33.7	985	0.47	25
CoHMA(0.005)	46.3	36.6	950	0.45	25
CoHMA(0.01)	46.7	37.5	975	0.50	26
CoHMA(0.02)	47.2	38.8	931	0.44	26
CoHMA(0.02)[d]	47.2	38.7	925	0.42	27
CoHMA(0.04)	47.6	41.9	900	0.42	28
MCM-41[c]	46.6	40.5	1080	0.80	30
Co/MCM-41(0.02)	46.8	43.3	850	0.65	31

[a] Numbers in parentheses indicate the nominal Co/[Al + P] or Co/Si ratios.
[b] Average unit cell parameter (a_0) calculated using $1/d^2 = 4/3(h^2 + hk + k^2/a^2)$.
[c] After used for cyclohexane oxidation.
[d] Cobalt-free sample.

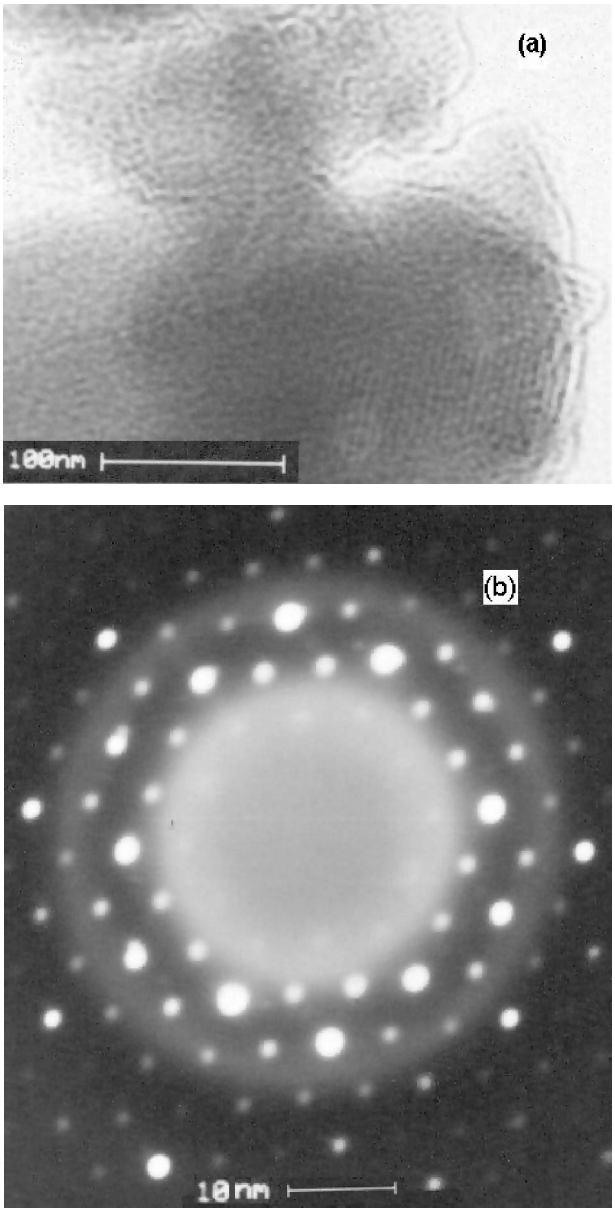

Fig. 2. TEM image (a); ED pattern (b) of calcined CoHMA(0.02).

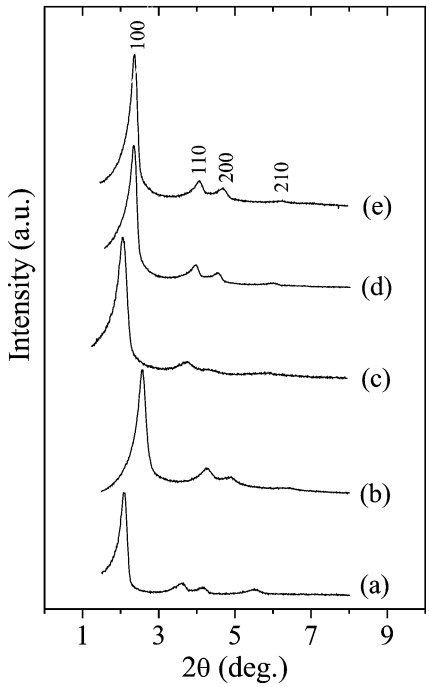

Fig. 3. XRD patterns of: (a) as-synthesized MCM-41; (b) calcined MCM-41; (c) as-synthesized Co/MCM-41; (d) calcined Co/MCM-41; (e) recycled Co/MCM-41.

or no increase in the lattice constant, even with a considerable increase in cobalt content. This indicates that the cobalt ions are not substituted in the tetrahedral framework of the silicate matrix. XRD patterns of CoAPO-5 ($a = 13.77$ Å, $c = 8.43$ Å) and Co/S-1 ($a = 20.10$ Å, $b = 19.99$ Å, and $c = 13.43$ Å) have shown that the samples are well crystallized, with AFI and MFI topologies [35,36].

TG of all of the as-synthesized CoHMA samples (not reproduced here) showed a total weight loss of 60–65% in three different stages, which is typical of mesoporous materials, corresponding to adsorbed water, occluded surfactant, and charge-compensating organic base [37]. On the other hand, the calcined CoHMA samples (not reproduced here) showed a weight loss in the 20–25% range due to the adsorbed water/gaseous molecules, with a corresponding endothermic transition at 383–393 K in DTA, indicating the mesoporous nature of the samples. The calcined Co-free HMA sample showed 18% weight loss. The hydrophilic nature of the CoHMA samples is due to the formation of acid sites generated by the incorporation of Co(II) for Al(III) ions.

The TG results are well supported by TPDA studies (Fig. 4). It can be seen from this figure that the desorption pattern of cobalt-free HMA consists of two distinct peaks concentrated at 443 and 873 K. The desorption peak at the lower temperature range mostly consists of P–OH or Al–OH defect sites in the matrix, corresponding to weak Brønsted acid sites. The peak at the higher temperature corresponds to the Lewis acid sites of the sample. Similarly weak Brønsted acid sites were also observed for the CoHMA profile [38–40]. In addition to the peaks observed for HMA, CoHMA shows a strong shoulder around 573–673 K, which corresponds to the structural Brønsted acid sites generated by the incorporation of Co^{2+} for Al^{3+}. This structural Brønsted acid sites are generated because of the charge difference between the Al^{3+} ion and the Co^{2+} ion, which replaced it in the process of substitution, because of which the lattice acquires a one-electron charge that must be compensated for by an extraframework cation for the stabilization of the matrix. In the as-synthesized sample the CTA^+ or TMA^+ acts as the extraframework cation, and after calcination, they give rise to a proton at the charge balancing cation. A similar type of observation is also reported for CoAPOn molecular sieves [41,42]. In microporous aluminophosphates it has been shown

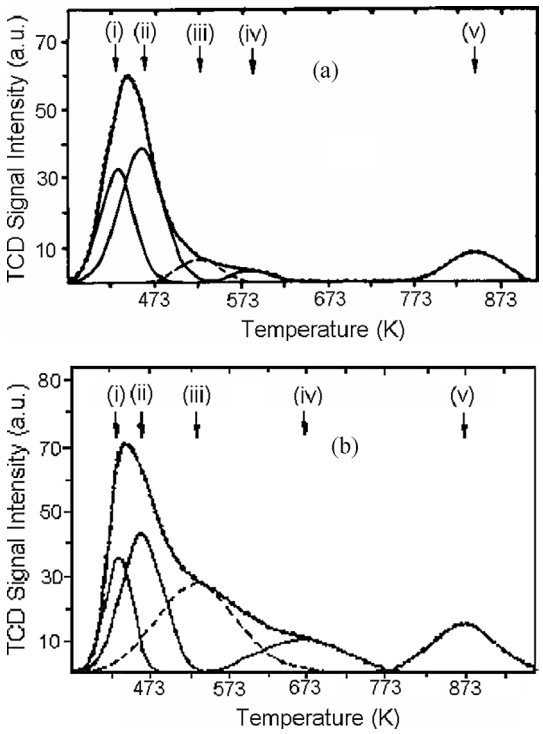

Fig. 4. Temperature-programmed desorption of ammonia of calcined samples: (a) HMA; (b) CoHMA(0.02).

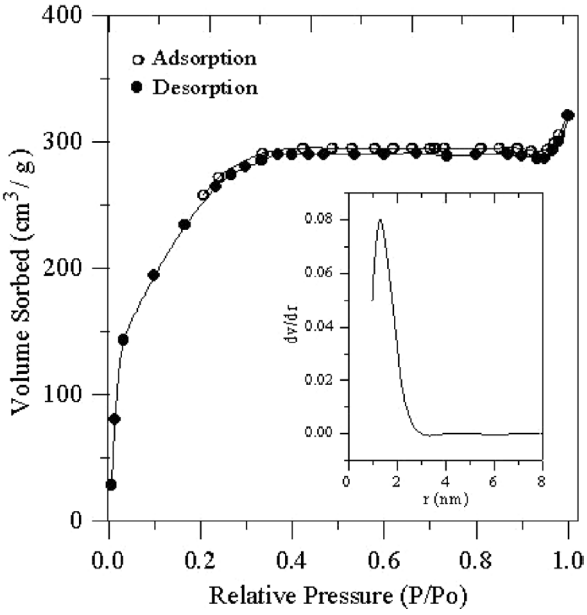

Fig. 5. N_2 sorption isotherms of calcined CoHMA(0.02). Inset: pore size distribution.

that by the partial hydrolysis of Al–O–P bonds, according to the reaction

$$\text{–Al–O–P–} + H_2O \leftrightarrow \text{–Al–OH} + \text{HO–P–},$$

weak Brønsted acid sites arise [43]. We expect that the same phenomenon is also occurring for mesoporous aluminophosphates. On the other hand, the peak at the higher temperature range may form because of the presence of tricoordinated aluminum or octahedral aluminum oxide or oxyhydroxide species present in the matrix due to incomplete condensation of the network [44]. It is also demonstrated in the literature that framework cobalt can also act as a Lewis acid center in cobalt-containing molecular sieves [45,46]. Deconvolution of the profiles of both HMA and CoHMA with the use of the Gaussian function with temperature as variant showed five peaks. The first two peaks (types I and II) are attributed to the weak Brønsted acid sites. Types III and IV correspond to the structural acid sites whose percentages are increased significantly from HMA (10%) to CoHMA (46.5%), indicating the incorporation of Co^{2+} in place of Al^{3+}. The type V curve is attributed to the Lewis acidic centers in the samples. In contrast, in the case of calcined Co/MCM-41, a decrease in weight loss observed for calcined Co/MCM-41 is about 10%, as compared with 18% MCM-41, thus suggesting the formation of extraframework species; that is, some of the silanol groups are consumed for the stabilization of cobalt ions in the matrix in a manner similar to that reported for (Cr)MCM-41 [47,48].

Nitrogen adsorption–desorption (sorption) studies confirmed the mesoporous nature of all of the samples (Table 1); a representative isotherm of CoHMA is presented in Fig. 5. It follows the type IV isotherm pattern typical of mesoporous materials [49]. As the relative pressure increases ($P/P_0 > 0.2$), the isotherm exhibits an inflection characteristic of capillary condensation within the mesopores. Adsorption at low relative pressures ($P/P_0 < 0.2$) is caused by monolayer adsorption of nitrogen on the walls of the mesopores. At $P/P_0 = 0.5$ the pore volume was calculated to be 0.44 $cm^3\,g^{-1}$ with SSA-BET, 931 $m^2\,g^{-1}$. A narrow pore size distribution was observed (Fig. 5, inset) with a mesopore diameter of 26 Å. These values are close to those of Co-free HMA samples (SSA-BET = 985 $m^2\,g^{-1}$; pore volume = 0.47 $cm^3\,g^{-1}$; pore size = 25 Å). On the other hand, calcined Co/MCM-41 showed a huge loss in surface area (SSA-BET = 850 $m^2\,g^{-1}$) compared with MCM-41 (SSA-BET = 1080 $m^2\,g^{-1}$), which supports the formation of extraframework cobalt species inside the pore and is in accordance with TG-DTA studies. Table 2 summarizes the ICP-AES results for calcined HMA and CoHMA. The increased Co/[Al + P] (molar) ratios in calcined samples as compared with the starting gel indicate that some of the aluminum and/or phosphorus may be lost in the mother liquor during the synthesis. The amount of cobalt varied in the following order: CoHMA > CoAPO-5 > Co/MCM-41 > Co/S-1.

Fig. 6 presents ^{27}Al-MAS-NMR spectra for as-synthesized and calcined CoHMA. It is interesting to note that the spectra for the as-synthesized and calcined samples exhibit two main resonances, ca. 53 and 13 ppm, which may correspond to tetrahedral $Al(OP)_4$ and octahedral $Al(OP)_4(H_2O)_2$, respectively [50,51]. Octahedral species in the as-synthesized form of mesoporous aluminophosphates is a common feature [29,52]. These findings suggest that the inorganic network of HMA consists not only of tetrahedral

Table 2
ICP-AES analysis of various cobalt-containing molecular sieves

Catalyst[a]	Al/P ratio	Co/[Al + P] ratio	Co/Si ratio	Co (wt%)
CoHMA(0.005)	1.30	0.006	–	0.90
CoHMA(0.01)	1.29	0.011	–	1.50
CoHMA(0.02)	1.27	0.022	–	3.80
CoHMA(0.04)	1.26	0.031	–	5.30
CoAPO-5(0.02)	0.98	0.021	–	3.20
Co/MCM-41(0.02)	–	–	0.016	2.30
Co/S-1(0.02)	–	–	0.0136	1.90

[a] Numbers in parentheses indicate the nominal Co/[Al + P] or Co/Si ratios.

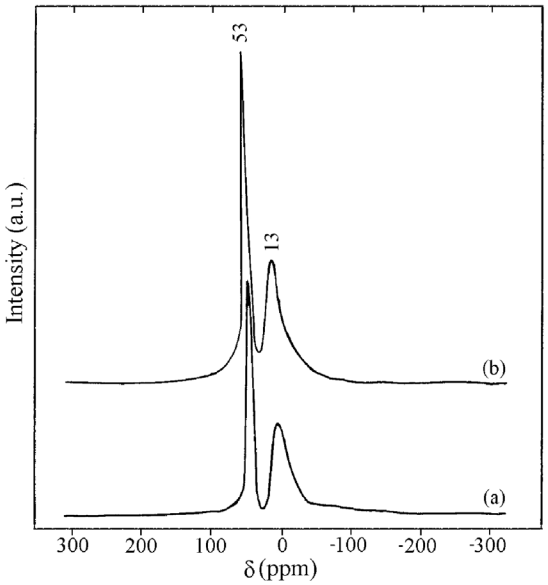

Fig. 6. ^{27}Al MAS-NMR of: (a) as-synthesized CoHMA(0.02); (b) calcined CoHMA(0.02).

aluminum, but also of tricoordinated aluminum and/or aluminum oxide/oxyhydroxide species in octahedral geometry [40,41,51]. It is also clear from the spectrum of the calcined sample that no further or very little dislodgement of aluminum occurs, but a slightly higher relative intensity of the octahedral resonance is noticed, which may be accounted for by the water coordination in lieu of nitrogen-containing surfactants.

All of the as-synthesized CoHMA samples were blue, and an increase in cobalt content in CoHMA results in a deep blue color, suggesting that the incorporated cobalt ions are in the divalent state with tetrahedral coordination geometry. It is quite interesting to note, however, that the color of CoHMA remains unchanged upon calcinations, indicating that the tetrahedrally inserted divalent cobalt ion is unaffected by the thermal treatment. These observations are further substantiated by DR-UV–vis studies, wherein both the as-synthesized and calcined CoHMA spectra exhibit triplet absorption bands (540, 580, and 626 nm) in the visible region (Fig. 7). They are assigned to the $^4A_2(F) \rightarrow {}^4T_1(P)$ transition of Co(II) in the tetrahedral environment of oxide

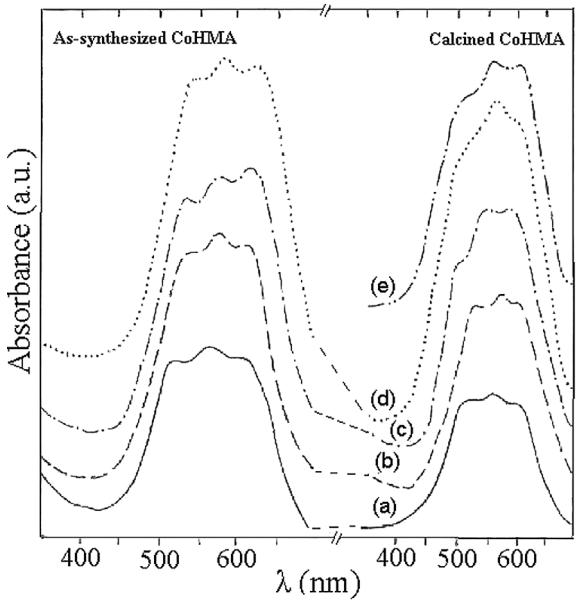

Fig. 7. DR-UV–vis spectra of: (a) CoHMA(0.005); (b) CoHMA(0.01); (c) CoHMA(0.02); (d) CoHMA(0.04); (e) recycled CoHMA(0.02).

ions [10,53]. A similar observation was reported earlier for microporous cobalt aluminophosphate molecular sieves with LTL topology [54]. However, these findings are in contrast with the familiar trend of microporous cobalt aluminophosphate molecular sieve systems such as CoAPO-5, wherein the blue color of the as-synthesized samples (triplet absorption bands in the visible region; see Fig. 8) turns to greenish-yellow upon calcination. This observation could possibly be attributed to a local distortion in the tetrahedral environment or dislodgement of cobalt ions. More importantly, upon calcination, no change in the spectral pattern was observed for CoHMA (Fig. 7), whereas CoAPO-5 shows a significant reduction in overall intensity of the visible triplet band, with the appearance of an additional new band in the UV region (Fig. 8). The band at 370 nm is, in general, assigned either to a transformation of symmetrical divalent tetrahedral cobalt to highly distorted tetrahedral coordination [55–57] or to a possible oxidation of divalent cobalt to trivalent cobalt [58–60]. On the other hand, the DR-UV–vis spectra of as-synthesized Co/MCM-41 and Co/S-1 (Fig. 8) showed characteristic transitions corresponding to divalent cobalt in octahedral coordination, which is in accordance with the observed pink color of the samples. However, upon calcination, the color of both Co/MCM-41 and Co/S-1 was changed to pinkish blue, which may be a consequence of the formation of cobalt oxide clusters [22]. This was indicated by the increase in the absorption band at the 580 and 620-nm transitions in the calcined samples compared with the as-synthesized samples (Fig. 8). It should to be noted here, however, that the cobalt-free samples are colorless, regardless of the structure types.

Fig. 9 presents XANES spectra for various cobalt-containing samples. For all of the samples, a large white line is observed, indicating a Co–oxygen interaction at a

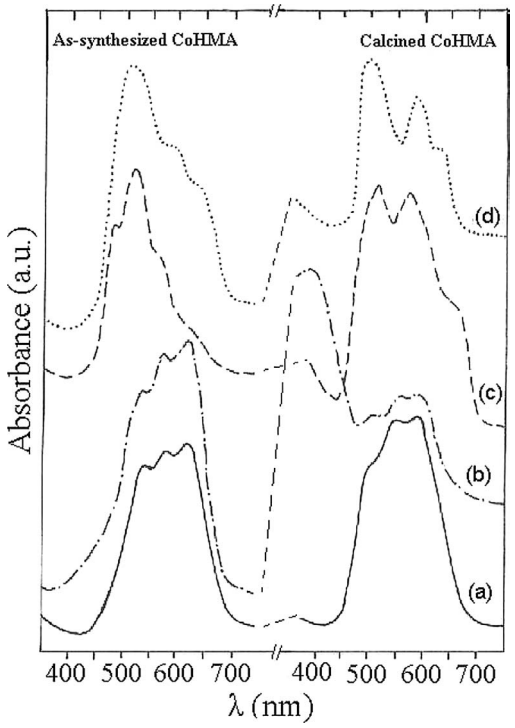

Fig. 8. DR-UV–vis spectra of: (a) CoHMA(0.02); (b) CoAPO-5; (c) Co/MCM-41; (d) (Co)/S-1.

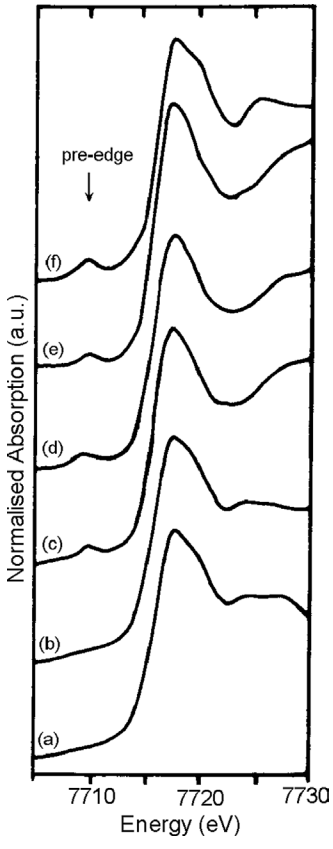

Fig. 9. Co K-edge XANES of: (a) as-synthesized Co/MCM-41; (b) calcined Co/MCM-41; (c) as-synthesized CoAPO-5; (d) calcined CoAPO-5; (e) as-synthesized CoHMA(0.02); (f) calcined CoHMA(0.02).

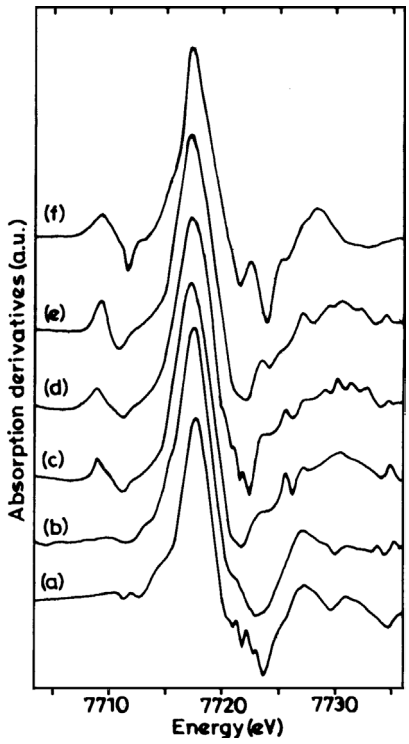

Fig. 10. First derivative Co K-edge XANES of: (a) as-synthesized Co/MCM-41; (b) calcined Co/MCM-41; (c) as-synthesized CoAPO-5; (d) calcined CoAPO-5; (e) as-synthesized CoHMA(0.02); (f) calcined CoHMA(0.02).

short distance. The spectra of as-synthesized CoHMA and CoAPO-5 show pre-edge peaks (7710 eV) associated with the dipole forbidden $1s \rightarrow 3d$ transition from the tetrahedral divalent cobalt, which becomes partially allowed because of p–d mixing in tetrahedral symmetry [61–63]. As expected, no significant change in pre-edge position was observed for the calcined samples, indicating that Co(II) ions remain in tetrahedral coordination in both CoHMA and CoAPO-5. On the other hand, as-synthesized Co/MCM-41 did not show any pre-edge peak, indicating that most of the cobalt species were in octahedral coordination. However, the calcined Co/MCM-41 showed a weak pre-edge, which was probably due to the formation of cobalt oxide clusters with tetrahedral Co–O linkages [22]. Fig. 10 shows the first derivative spectra of all of the cobalt-containing samples. The peak at 7722 eV for all of the cobalt-containing aluminophosphate samples indicates the presence of trivalent cobalt in octahedral coordination. This might have arisen because of the formation of amorphous $CoAl_2O_4$-type species [63]. This was not observed for silicate matrixes.

Table 3 shows the catalytic oxidation results for cyclohexane over various cobalt-containing HMA catalysts. It is well known that the use of initiators shortens the induction period and enhances the catalytic activity significantly [47], as a result of the formation of chelate complex, which may easily be cleaved into free radicals capable of initiating chain transfer by hydrogen abstraction with cyclohexane. Hence in the present investigation we have used

Table 3
Effect of cobalt concentration in CoHMA catalyst on the oxidation of cyclohexane[a]

Catalyst	Conversion (wt%)	Selectivity (wt%)		
		-ol	-one	others
CoHMA(0.005)	78.6	97.0	2.0	1.0
CoHMA(0.01)	81.2	94.6	2.9	2.5
CoHMA(0.02)	90.7	93.4	4.8	1.8
CoHMA(0.04)	99.1	80.3	17.7	2.0

[a] Reaction conditions: substrate:oxidant (H_2O_2) = 1:1; catalyst = 50 mg (3.3 wt%); solvent = acetic acid (10 ml); MEK = 5 mmol; temperature = 373 K; time = 12 h.

Table 4
Oxidation of cyclohexane over various cobalt containing catalysts[a]

Catalysts	Conversion (wt%)	Co content[b] (wt%)	Selectivity (wt%)		
			-ol	-one	others
CoHMA(0.02)					
Calcined	90.7	3.80	93.4	4.8	1.8
Filtrate	12.5	0.19	89.5	4.5	6.0
Quenched solution	10.8	–	87.0	6.8	6.2
Recycled[c]	86.8	3.61	88.9	9.4	1.7
Washed	87.1	3.65	88.6	9.5	1.9
HMA	9.8	–	82.8	1.3	15.9
Co/MCM-41					
Calcined	68.7	2.30	87.1	8.7	4.2
Filtrate	32.8	1.10	82.4	12.0	5.6
Quenched solution	30.0	–	84.0	9.8	6.2
Recycled[c]	40.7	1.20	86.7	10.8	2.5
Washed	45.2	1.30	88.0	8.7	3.3
CoAPO-5					
Calcined	78.9	3.20	81.6	17.3	6.1
Recycled	50.8	2.62	80.2	15.1	4.7
Co/S-1	41.2	1.90	85.7	6.7	7.6
MCM-41	11.6	–	96.4	–	3.6
Blank	9.0	–	78.1	–	21.9
CoO	28.3	78.60	79.4	10.0	10.6
$Co(CH_3COO)_2{\cdot}4H_2O$	95.0	23.65	44.0	38.0	18.0

[a] Reaction conditions: substrate:oxidant (H_2O_2) = 1:1; catalyst = 50 mg (3.3 wt%); solvent = acetic acid (10 ml); MEK = 5 mmol; temperature = 373 K; time = 12 h.
[b] From ICP-AES analysis.
[c] 3rd recycle or 4th run.

MEK as the initiator. All of the catalysts showed two major products, cyclohexanol (-ol) and cyclohexanone (-one). Of the other by-products, cyclohexyl acetate was detected, which forms because of the chain termination process between the cyclohexyl and acetate free radical. Table 3 shows that with increasing cobalt amount in the catalyst, the cyclohexane conversion increases and the cyclohexanol selectivity decreases, because of the overoxidation of cyclohexanol to cyclohexanone. In the case of high-cobalt-content (5.3 wt%) catalyst, CoHMA(0.04), the highest amount of cyclohexanone formation was observed. It should also be noted here that HMA, without catalyst (blank), and CoO catalyst show meager activity (10–20% conversion) (Table 4). Thus, the observed high activity and selectivity of CoHMA catalysts could be attributed to the presence of isolated tetrahedral Co^{2+} in the HMA matrix, under optimized mild reaction conditions: acetic acid as solvent, MEK as initiator, H_2O_2 as oxidant at 373 K for 12 h [37]. All of the studies were carried out for the catalyst CoHMA. The use of solvents like THF, methanol, and acetone did not show any activity. Thus the use of acetic acid as the solvent is essential, as it helps in the oxidation of the active species Co^{2+} to Co^{3+} in the presence of the oxidant and initiator [5,64]. The reaction was also carried out with different oxidants: 70% TBHP, molecular O_2, and air; the results are listed in Table 5. The reaction with H_2O_2 exhibits high conversion at high cyclohexanol selectivity. With an increased amount of H_2O_2, almost complete oxidation (99.6%) of cyclohexane can be possible at 78% cyclohexanol and 17% cyclohexanone (Fig. 11). Reddy et al. [65] also observed the increase in cyclohexanone selectivity, with an increase in the H_2O_2 amount for the TS-2 catalyst. On the other hand, TBHP gave cyclohexanone as the major product, since this oxidant is more reactive than H_2O_2 [66]. However, the conversion was lower than with H_2O_2, which may be due to the deactivation of the catalyst by the formation of *tert*-butanol from the decomposition of TBHP. When the reaction was carried out by molecular O_2 and air, it led to low substrate conversion with cyclohexanol as the major

Table 5
Effect of different oxidants on the oxidation of cyclohexane over CoHMA(0.02) catalyst[a]

Oxidant	Conversion (wt%)	Selectivity (wt%)		
		-ol	-one	others
H_2O_2 (30%)	90.7	93.4	4.8	1.8
TBHP (70%)	78.8	28.0	68.0	4.0
O_2	52.2	94.0	3.2	2.8
Air	42.5	96.5	1.0	2.5

[a] Reaction conditions: substrate:oxidant (H_2O_2 or TBHP) = 1:1; air and O_2 flow = 40 ml min^{-1} catalyst = 50 mg (3.3 wt%); solvent = acetic acid (10 ml); MEK = 5 mmol; temperature = 373 K; time = 12 h.

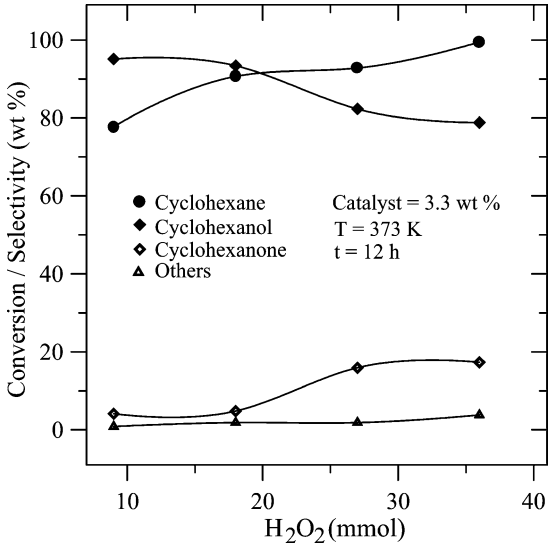

Fig. 11. Effect of H_2O_2 concentration on the oxidation of cyclohexane over CoHMA(0.02).

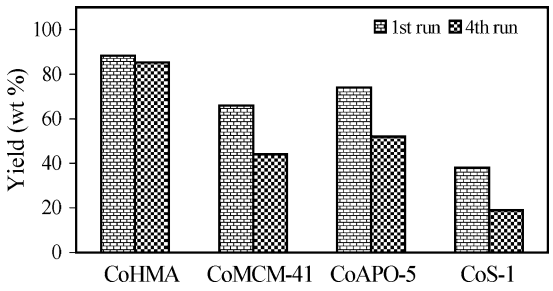

Fig. 12. Recycling results of various cobalt-containing catalysts for the oxidation reaction of cyclohexane.

product. This may be due to the fact that the direct attack of O_2 on cyclohexane is an endothermic process, thus creating difficulties in the activation of a process. To overcome this problem, various other oxidants, such as idosobenzene [67,68], hydrogen peroxide [69–72], and alkylhydroperoxide [73,74], have been used instead of energy-consuming dioxygen activation. H_2O_2 is a preferable oxidant because of its simplicity of handling, the environmentally friendly nature of the coproduct (water), the high oxygen atom efficiency, and its versatility [75–77].

To check the reusability of the catalyst, recycling and washing experiments were carried out. It is interesting to note here that a meager loss in activity was observed after the fourth run. This clearly indicates that most of the cobalt ions are intact in the framework, which was confirmed by ICP-AES analysis of the filtrate, where a very small amount of cobalt (0.19 wt%) was noticed as compared with the high cobalt level (3.8 wt%) present in the catalyst. Some leaching might have occurred because of the presence of a small amount of loosely bound extraframework cobalt species in the matrix. Moreover, the reaction was also performed on the filtrate and the quenched solution, which showed only a meager activity, thus suggesting CoHMA to be a truly heterogeneous catalyst, and the activity is not significantly contributed to, because of the small loss of cobalt in reaction conditions. This is well supported by the DR-UV–vis spectra of treated catalysts (Fig. 7e), where no major change in intensity of the triplet band/color change was noticed. We further confirmed this by performing the reaction over ammonium acetate-washed CoHMA catalyst, where the activity observed was comparable to that of the calcined catalyst. Furthermore, the structure (Fig. 1) and porosity (Table 1) remained unaltered, even after various treatments. This indicates the stability of the catalysts under the mild reaction conditions used.

The reaction was also carried out over Co/MCM-41, CoAPO-5, and Co/S-1; the results are shown in Table 4 and Fig. 12. It can be seen from the table that the order of activity is CoHMA > CoAPO-5 > Co/MCM-41 > Co/S-1. Co/S-1 showed the least activity, because of its small pore opening, which hinders the diffusion of the substrate molecules inside the pore aperture, compared with other catalysts. It is well known that bulk metal oxides generally decompose hydrogen peroxides, which thus decreases the efficiency of the

Table 6
Oxidation of cyclooctane over various cobalt containing catalysts[a]

Catalysts	Conversion (wt%)	Selectivity (wt%)		
		-ol	-one	others
CoHMA(0.02)				
Calcined	92.4	85.0	11.5	3.5
Recycled[b]	90.8	81.5	14.8	3.7
Co/MCM-41	58.2	77.0	10.0	13.0
CoAPO-5	33.5	68.0	15.7	16.3
Co/S-1	28.0	74.0	11.3	14.7

[a] Reaction conditions: substrate:oxidant (H_2O_2) = 1:1; catalyst = 50 mg (2.48 wt%); solvent = acetic acid (5 ml) + CH_2Cl_2 (5 ml); MEK = 5 mmol; temperature = 373 K; time = 12 h.

[b] 3rd recycled or 4th run.

oxidant in an oxidation process, and this may be the cause for the lower activity of Co/MCM-41 (68.7% conversion) compared with CoHMA(0.02) [78]. The activity also decreased with recycling, with a considerable amount of cobalt leached (1.1%) to the reaction mixture.

On the other hand, CoAPO-5 showed 78.9% conversion. The low activity may be attributed to low cobalt content (3.2 wt%). In addition, the catalyst also lost its activity (50.8% conversion after the fourth run) because of leaching of active cobalt ions (0.58 wt%) under reaction conditions, which is very well supported by the filtrate experiments, where the leached cobalt ions showed considerable activity (35.8% conversion). Furthermore, these results are in good agreement with the DR-UV–vis studies (not reproduced here) on the recycled catalyst, where the two additional bands, which normally appear for the calcined CoAPO-5 because of the highly distorted tetrahedral environment of Co^{2+}/Co^{3+}, disappear. Fig. 12 indicates the yield of cyclohexanol and cyclohexanone, which remains almost same for CoHMA, but a significant decrease is observed for Co/MCM-41, CoAPO-5, and Co/S-1 catalysts.

At this juncture, it is also important to note that the reaction was also carried out with traditional cobalt(II) acetate (homogeneous) catalyst under our reaction (mild) conditions. Although it gives very high substrate conversion (∼ 95%), the selectivity for cyclohexanol is very low (∼ 44%). Furthermore, it also produces several unidentified products. In contrast, the mesoporous CoHMA (heterogeneous) catalyst gives high cyclohexane conversion (90%) and excellent cyclohexanol selectivity (93%). Hence, this opens up new avenues in cyclohexane oxidation over conventional catalysts. Furthermore, the results also indicate that secondary oxidation of cyclohexanol and CoHMA can control cyclohexanone to waste products very well, which is normally observed under homogeneous conditions.

To exploit the mesoporosity of the CoHMA catalyst, the oxidation of bulkier cycloalkanes, that is, cyclooctane (Table 6) and cyclododecane (Table 7), was also carried out. It is interesting to note that CoHMA showed excellent activity for these bulkier substrates compared with Co/MCM-41, CoAPO-5, and Co/S-1. CoAPO-5 and Co/S-1

Table 7
Oxidation of cyclododecane over various cobalt containing catalysts[a]

Catalysts	Conversion (wt%)	Selectivity (wt%)		
		-ol	-one	others
CoHMA(0.02)				
Calcined	89.8	77.0	17.1	5.9
Recycled[b]	86.0	75.5	20.0	4.5
Co/MCM-41	48.8	65.0	18.0	17.0
CoAPO-5	28.0	68.3	15.2	16.5
Co/S-1	23.0	72.5	12.0	15.5

[a] Reaction conditions: substrate:oxidant (H_2O_2) = 1:1; catalyst = 50 mg (2.48 wt%); solvent = (5 ml acetic acid + 5 ml CH_2Cl_2); MEK = 5 mmol; temperature = 373 K; time = 12 h.

[b] 3rd recycled or 4th run.

showed only meager activity because of their pore size restriction for these bulky substrates. The lower activity of Co/MCM-41 was accounted for by the clustering of cobalt species inside the pores, which was not favorable for the oxidation reactions. CoHMA showed good recyclability for these substrates as well. The XRD pattern remained unaltered after reuse. In a comparison of the results for cyclohexane oxidation with those for these substrates, it was observed that more ketone (cyclooctanone and cyclododecanone) was formed in bulkier substrates, resulting in a decrease in selectivity of the alcohols (cyclooctanol and cyclododecanol). The decrease in alcohol selectivity may be accounted for by the lower diffusion rate of the bulky cyclooctanol/cyclododecanol compared with cyclohexanol inside the mesopores, which leads to the overoxidation of the alcohols to ketones.

4. Conclusion

In conclusion, the successful synthesis and characterization of Co^{2+}-substituted hexagonal mesoporous aluminophosphate molecular sieves were achieved. Unlike many other cobalt-based heterogeneous systems, the cobalt ions did not change their color/environment during calcination. The CoHMA catalysts showed excellent activity for selective oxidation of cyclohexane under mild reaction conditions. The activity of CoHMA(0.02) was found to be higher than those of the Co/MCM-41, CoAPO-5, and Co/S-1 catalysts. It was also demonstrated that CoHMA can be used for the oxidation of bulky cycloalkanes, such as cyclooctane and cyclododecane. These catalysts can be considered viable alternatives because of their easy recovery and recycling; thus they open up a new possibility for heterogeneous oxidation reactions.

Acknowledgments

The authors thank RSIC/SAIF, IIT-Bombay, for ICP-AES, TEM, and ED measurements. Thanks are also due to Dr. A. Sakthivel and Dr. S. Balamurugan for their experimental assistance.

References

[1] K. Tanaka, Hydrocarbon Proc. 53 (1974) 114.
[2] A. Onopchenko, J.G.D. Schulz, J. Org. Chem. 38 (1973) 3729;
A. Onopchenko, J.G.D. Schulz, J. Org. Chem. 40 (1975) 3338.
[3] D.G. Hendry, C.W. Gould, D. Schuetzle, M.G. Syz, F.R. Mayo, J. Org. Chem. 41 (1976) 1.
[4] R.A. Sheldon, J.K. Kochi, Metal Catalysed Oxidation of Organic Compounds, Academic Press, New York, 1981.
[5] G.W. Parshall, S.D. Ittel, Homogeneous Catalysis, Wiley, New York, 1992.
[6] S.-I. Murahashi, T. Naota, N. Komiya, Tetrahedron Lett. 36 (1995) 8059.
[7] H. Tang, C. Shen, M. Lin, A. Sen, Inorg. Chem. Act. 300–302 (2000) 1109.
[8] W.B. Fisher, J.F. Vanpappen, A.S. Inc, in: M. Howe-Grant, J.I. Kroschwitz (Eds.), Cyclohexanol and Cyclohexanone, in: Kirk–Othmer Encyclopedia of Chemical Technology, vol. 7, Wiley, New York, 1992, p. 851.
[9] P. Battioni, R. Iwanejko, D. Mansuy, T. Mlodnicka, J. Poltowicz, F. Sanchez, J. Mol. Catal. A 109 (1996) 91.
[10] A.A. Verberckmoes, B.M. Weckhuysen, R.A. Schoonheydt, Micropor. Mesopor. Mater. 22 (1998) 165.
[11] R. Mostowicz, A.J. Dabrowski, J.M. Jablonski, Stud. Surf. Sci. Catal. 49A (1989) 249.
[12] T. Inui, J.-B. Kim, T. Takeguchi, Zeolites 17 (1996) 354.
[13] C.I. Round, C.D. Williams, C.V.A. Duke, Chem. Commun. (1997) 1849.
[14] B. Kraushaar-Czarnetzki, W.G.M. Hoogervorst, W.H.J. Stork, Stud. Surf. Sci. Catal. 84 (1994) 1869.
[15] S.S. Lin, H.S. Weng, Appl. Catal. A 105 (1993) 289;
S.S. Lin, H.S. Weng, Appl. Catal. A 118 (1994) 21;
S.S. Lin, H.S. Weng, J. Chem. Eng. Jpn. 27 (1994) 211.
[16] D.L. Vanoppen, D.E. De Vos, M.J. Genet, P.G. Rouxhet, P.A. Jacobs, Angew Chem. Int. Ed. Engl. 34 (1995) 560.
[17] P. Conception, A. Corma, J.M.L. Nieto, J. Perez-pariente, Appl. Catal. A 143 (1996) 17.
[18] F.J. Luna, S.E. Ukawa, M. Wallau, U. Schuchardt, J. Mol. Catal. A 117 (1997) 405.
[19] I. Belkhir, A. Germain, F. Fajula, E. Fache, J. Chem. Soc., Faraday Trans. 94 (1998) 1761.
[20] G. Sankar, R. Raja, J.M. Thomas, Catal. Lett. 55 (1998) 15.
[21] A.F. Masters, J.K. Beattie, A.L. Roa, Catal. Lett. 75 (2001) 159.
[22] A. Jentys, N.H. Pham, H. Vinek, M. Englisch, J.A. Lercher, Micropor. Mater. 6 (1996) 13.
[23] D.H. Park, S.S. Park, S.J. Choe, Bull. Korean Chem. Soc. 20 (1999) 715.
[24] J. Vinu, J. Dedecek, V. Murugesan, M. Hartmann, Chem. Mater. 14 (2002) 2433.
[25] T. Maschmeyer, R.D. Oldroyd, G. Sankar, J.M. Thomas, I.J. Shannon, J.A. Klepetko, A.F. Masters, J.K. Beattie, C.R. Catlow, Angew Chem. Int. Ed. Engl. 36 (1997) 1639.
[26] M. Nowotny, L.N. Pedersen, U. Hanefeld, T. Maschmeyer, Chem. Eur. J. 8 (2002) 3724.
[27] T. Kimura, Micropor. Mesopor. Mater. 77 (2005) 97, and references are cited therein.
[28] A. Sakthivel, N. Arunkumar, P. Selvam, Bull. Catal. Soc. India 1 (2002) 136.
[29] T. Kimura, Y. Sugahara, K. Kuroda, Chem. Commun. (1998) 559;
T. Kimura, Y. Sugahara, K. Kuroda, Chem. Mater. 11 (1999) 508.
[30] P. Selvam, S.K. Bhatia, C.G. Sonwane, Ind. Eng. Chem. Res. 40 (2001) 3237.

[31] P.T. Tanev, T.J. Pinnavaia, Science 267 (1995) 865.
[32] S.A. Bagshaw, E. Prouzet, T.J. Pinnavaia, Science 269 (1995) 1242.
[33] R. Ryoo, J.M. Kim, C.H. Ko, J. Phys. Chem. 100 (1996) 17718.
[34] J.S. Beck, J.C. Vartuli, W.J. Roth, M.E. Leonowicz, K.D. Schmidtt, C.T.-W. Chu, D.H. Olson, E.W. Sheppard, S.B. McCullen, J.B. Higgins, J.L. Schlenker, J. Am. Chem. Soc. 114 (1992) 10834.
[35] J.M. Bennett, J.P. Cohen, E.M. Flanigen, J.J. Pluth, J.V. Smith, ACS Sym. Ser. 218 (1983) 109.
[36] G.T. Kokotailo, S.L. Lawton, D.H. Olson, W.H. Meier, Nature 272 (1978) 437.
[37] S.K. Mohapatra, P. Selvam, Top. Catal. 22 (2003) 17.
[38] D. Arias, I. Campos, D. Escalante, J. Goldwasser, C.M. Lopez, F.J. Machado, B. Mendez, D. Moronta, M. Pinto, V. Sazo, M.M.R. de Agudelo, J. Mol. Catal. A 122 (1997) 175.
[39] E. Dumitriu, V. Hulea, I. Fechete, A. Auroux, J.-F. Lacaze, C. Guimon, Micropor. Mesopor. Mater. 43 (2001) 341.
[40] J. Das, C.V.V. Satyanaryana, D.K. Chakrabarty, S.N. Piramanayagam, S.N. Shringi, J. Chem. Soc., Faraday Trans. 88 (1992) 3255.
[41] N.J. Tapp, N.B. Milestone, L.J. Wright, Chem. Commun. (1985) 1801.
[42] U. Lohse, R. Bertram, K. Jancke, I. Kurzawski, B. Parlitz, E. Loffler, E. Schreier, J. Chem. Soc., Faraday Trans. 91 (1995) 1163.
[43] B. Parlitz, U. Lohse, E. Schreier, Micropor. Mater. 2 (1994) 223.
[44] H. Kosslick, G. Lischke, H. Landmesser, B. Parlitz, W. Storek, R. Fricke, J. Catal. 176 (1998) 102.
[45] M.P.J. Peeters, J.H.C. van Hoof, R.A. Sheldon, V.L. Zholobenko, L.M. Kustov, V.B. Kazansky, in: R. von Ballmoos, J.B. Higgins, M.M.J. Treacy (Eds.), in: Proceeding of the 9th IZC, vol. I, Butterworth–Heinemann, Washington, DC, 1993, p. 651.
[46] L. Marchese, J. Chen, J.M. Thomas, S. Coluccia, A. Zecchina, J. Phys. Chem. 98 (1994) 13350.
[47] A. Sakthivel, P. Selvam, J. Catal. 211 (2002) 134.
[48] M.W. Anderson, C.C. Egger, G.J.T. Tiddy, J.L. Casci, Stud. Surf. Sci. Catal. 142B (2002) 1149.
[49] S. Storck, H. Bretinger, W.F. Maier, Appl. Catal. A 174 (1998) 137.
[50] M. Schultz, M. Tiemann, M. Froba, C. Jager, J. Phys. Chem. B 104 (2000) 10473.
[51] M. Froba, M. Tiemann, Chem. Mater. 10 (1998) 3475;
M. Froba, M. Tiemann, Chem. Mater. 13 (2001) 3217;
M. Froba, M. Tiemann, Chem. Commun. (2002) 406.
[52] Y.J. Khimyak, J. Klinowski, J. Mater. Chem. 12 (2002) 1079.
[53] F.A. Cotton, D.M.L. Goodgame, M. Goodgame, J. Am. Chem. Soc. 88 (1961) 4690.
[54] C. Montes, A.L. Villa, M.M. Ramirez-Corredores, Appl. Catal. A 197 (2000) 151.
[55] V. Kurshev, L. Kevan, D.J. Parillo, C. Pereira, G.D. Kokotailo, R.J. Gorte, J. Phys. Chem. 98 (1994) 10160.
[56] S. Thomson, V. Luca, R. Howe, Phys. Chem. Chem. Phys. 1 (1999) 615.
[57] B.M. Weckhuysen, A.A. Verberckmoes, M.G. Uytterhoeven, F.E. Mabbs, D. Collison, E. Boer, R.A. Schoonheydt, J. Phys. Chem. B 104 (2000) 37.
[58] L.E. Iton, I. Choi, J.A. Desjardins, V.A. Maroni, Zeolites 9 (1989) 535;
C. Montes, M.E. Devis, B. Murray, M. Narayana, J. Phys. Chem. 94 (1990) 6425.
[59] P.S. Singh, R.A. Shaikh, R. Bandyopadhyay, B.S. Rao, J. Chem. Soc., Chem. Commun. (1995) 2255.
[60] A. Frache, E. Gianotti, L. Marchese, Catal. Today 77 (2003) 371.
[61] G. Zhang, T.V. Harris, Physica B 208–209 (1995) 697.
[62] P.A. Barrett, G. Sankar, C.R.A. Catlow, J.M. Thomas, J. Phys. Chem. 100 (1996) 8977.
[63] A. Moen, D.G. Nicholson, M. Ronning, G.M. Lamble, J.-F. Lee, H. Merich, J. Chem. Soc., Faraday Trans. 93 (1997) 4071.
[64] J.F. Black, J. Am. Chem. Soc. 100 (1998) 527.
[65] J.S. Reddy, S. Sivasanker, Catal. Lett. 11 (1991) 241.
[66] E.L. Pires, J.C. Magalhaes, U. Schuchardt, Appl. Catal. A 203 (2000) 231.
[67] J.T. Groves, T.E. Nemo, J. Am. Chem. Soc. 105 (1983) 6243.
[68] T.G. Traylor, J.S. Buyn, P.S. Trylor, P. Battoni, D. Mansuy, J. Am. Chem. Soc. 113 (1991) 7821.
[69] J. Xiao, J. Xu, Z. Gao, Catal. Lett. 57 (1999) 37.
[70] C. Sheu, S.A. Richert, P. Cofre, B.J. Ross, A. Sobkowiak, D.T. Sawyer, J.R. Kanotsky, J. Am. Chem. Soc. 112 (1990) 1936.
[71] A.S. Goldstein, R.H. Beer, R.S. Drago, J. Am. Chem. Soc. 116 (1994) 2424.
[72] N. Mizuno, C. Nozaki, I. Kiyoto, M. Misono, J. Am. Chem. Soc. 120 (1998) 9267.
[73] R.F. Parton, G.J. Peere, P.E. Neys, P.A. Jacobs, R. Claessens, G.V. Baron, J. Mol. Catal. A 113 (1996) 445.
[74] P.A. Mac, I.W. Faul, C.E. Arends, K.U. Ingold, D.D.M. Wayner, J. Chem. Soc., Perkin Trans. 2 (1997) 135.
[75] R.A. Sheldon, Top. Curr. Chem. 164 (1993) 23.
[76] P. Knops-Gerrits, D.D. Vos, F. Thibault-Starzyk, P.A. Jacobs, Nature 369 (1994) 543.
[77] C.L. Hill, C.M. Prosser-McCartha, Coord. Chem. Rev. 143 (1995) 407.
[78] Y. Wang, Q. Zhang, T. Shishido, K. Takehira, J. Catal. 209 (2002) 186.